

# Microscopic Images Improvement Depending on Dark Channel Prior and Adaptive Histogram Equalization Based on the Lab Colour Model

Kahttan A. Noman<sup>1\*</sup>, Alauldeen Salah Yaseen<sup>2</sup>

<sup>1</sup> Presidency of the Council of Ministers in Iraq, Office of the Prime Minister's Advisor for Education, Tourism and Antiquities Affairs, Baghdad, Iraq

<sup>2</sup> Department of Applied Sciences, University of Technology, Baghdad, Iraq

\* Corresponding author's e-mail: aljbouirqahtan@gmail.com

## ABSTRACT

Optical microscopes face limitations due to diffraction, which can impact the clarity and resolution of the resulting images. Enhancing these images typically involves techniques such as contrast improvement, sharpening, and noise reduction, which help make features more discernible. In this study, we propose an algorithm aimed at enhancing contrast and illumination using dark channel prior (DCP) and adaptive histogram equalization (AHE) to improve image clarity. For illumination enhancement, we utilize the lab colour model, specifically focusing on the light formation component (L) while preserving colour. This method was compared against several others, including the Retinex algorithm with colour restoration, adaptive histogram equalization and fuzzy logic, fuzzy logic by stretch membership function, median-mean based sub-image-clipped histogram equalization, principal component analysis using reflection model, and modified colour histogram equalization, using both reference and non-reference quality standards. Our algorithm aims to enhance image contrast and brightness without introducing colour distortion, achieving favorable values for entropy (7.913), mean of the standard deviation (61.04), structural similarity index metric (0.760), and perception-based image quality evaluator (35.324).

**Keywords:** DCP, microscope image enhancement, (Lab) colour space, colour restoration.

## INTRODUCTION

One of the branches of image processing, image enhancement has a variety of uses [1] such as images from medical optical microscopy [2], object detection [3], recognition [4], and dehazing images [5]. Techniques for processing images can be separated into two categories. The first is spatial image processing performed by changing the pixel. The second is frequency-domain image processing, which includes discrete, Fourier, wavelet, and cosine transform [4]. Images captured through optical microscopy play a pivotal role across various domains. In scientific research, they offer insights into intricate natural and microscopic occurrences, such as cellular structures, microbial entities, and viral compositions. This aids in the exploration of biological and chemical

phenomena at a minute scale. In medical diagnostics, these images are instrumental in scrutinizing medical specimens like blood, tissues, and organs, facilitating the identification and comprehension of diverse ailments and their progression. Within pharmaceutical and food sectors, optical microscopy serves to scrutinize products, ensuring their quality and safety, while also overseeing industrial processes. Environmental science benefits from these images by delving into microenvironments, analyzing elements like soil, water, and organic substances, thereby shedding light on the impacts of pollution and environmental shifts. Across industrial and technological spheres, optical microscopy aids in the examination and analysis of materials and technologies at a micro scale, driving advancements in product development and industrial processes, in essence, images

obtained via optical microscopy are indispensable in scientific research and numerous technical applications, providing invaluable assistance in understanding precise phenomena, diagnosing diseases, and advancing technologies and products. The purpose of this study is to enhance the optical microscopy images. Contrast enhancement is a commonly used approach in computer vision, pattern recognition, and image processing applications [1]. This method's main objective is to make interesting objects more visible in order to support automated or user-oriented operations such as segmentation, analysis, detection, and recognition of objects. Daway et al. [6] proposed an algorithm to improve X-ray images. A contrast enhancement algorithm was presented using the Retinex algorithm based on retinex algorithm with colour restoration (RACR). The MSR algorithm was also used to increase the quality of lighting and contrast. This method includes several steps. First, they inserted X-ray images. Second, they applied contrast enhancement to each channel (R, G, and B) by using colour restoration and finally applying MSR to get an improved final image. This method was compared with several others (MRINE, CEDNI, MSRCR, and HE) using the entropy quality measure EN and histogram analysis. This method succeeded in increasing the contrast of X-rays. Zhou et al. [7] presented a method for improving the colour of retinal images to help doctors more efficiently examine eye diseases. as their method included improving the luminance and contrast of the images. To increase the R, G, and B (red, green, and blue) channels, respectively, the brightness gain matrix is generated by gamma correction of the value channel in the HSV colour space (hue, saturation, and value), and the contrast in the luminance channel is improved. For the colour space  $L^*a^*b^*$  by CLAHE, this method achieved superiority compared to other improvement methods as it preserved the nature of the image.

Wei and Ching [8] suggested histogram equalization serves as a pivotal method in image enhancement, using modified colour histogram equalization (MCHE) By crucially elevating image contrast, and has found indispensable utility in both general and medical image processing realms. Despite its widespread study and application, conventional histogram equalization tends to yield subpar image enhancement outcomes due to its oversight in preserving hue. Neha and Ashish [9] Introduction principal component analysis

using reflection model (PCAURM), in this algorithm dynamically adjusts for low-light images using a combination of reflection modeling and multiscale principles. Initially, an input RGB colour image undergoes colour correction and conversion to HSV colour space to address any colour distortions. Leveraging multiscale theory, the algorithm computes the illumination coefficient of the V component. Subsequently, a brightness enhancement technique, inspired by the Fechner principle, is applied, with adaptive parameter adjustment. Additionally, a PCA-based image fusion method is employed to extract pertinent features from these enhanced images. Finally, to enhance global contrast, the algorithm utilizes the contrast-limited adaptive histogram equalization (CLAHE) model.

Singh and Kapoor [10] suggested median-mean based sub-image-clipped histogram equalization (MMBSICHE) algorithm, In this method comprises three main stages: firstly, it computes the median and mean brightness values of the image; secondly, it clips the histogram using a plateau limit determined by the median of the occupied intensity; thirdly, it divides the clipped histogram into two halves based on median intensity and further splits it into four sub-images according to individual mean intensity. Afterward, histogram equalization is applied to each sub-image. This approach accomplishes multiple objectives – it maintains brightness and image information content (entropy) while also offering control over the enhancement rate, making it suitable for applications in consumer electronics. In [11] they proposed an approach using adaptive histogram equalisation and fuzzy logic (AHEFL) began by refining the image through contrast-limited adaptive histogram equalization (CLAHE). Subsequently, enhancement of the luminance channel within the colour space was conducted through sigmoid transformation and fuzzy logic. A dataset comprising 50 medical microscopy images was examined, and the efficacy of the proposed enhancement method was evaluated against several others. These included principal component analysis utilizing the reflection model, fuzzy logic employing stretch membership function, CLAHE, modified colour histogram equalization, contrast enhancement based on median-mean sub-image clipped histogram equalization and the retinex method with colour restoration. Comparative analysis revealed that the suggested method yielded commendable

quality improvements. In this study, we aim to improve microscopic images using adaptive histogram equalization (AHE) and dark channel prior (DCP) to improve image contrast and using the Lab colour model. We improved the lighting component L by using AHE separately from the colour components. The proposed method succeeded in improving microscopic images without causing any colour distortions.

### PROPOSED METHOD

In this study, we improve microscopic images based on the DCP and AHE algorithms in addition to the lab colour model. The image contrast is improved using DCP and AHE, and to improve the lighting component, we extract the lighting component L and improve it by using AHE. Figure 1 shows a diagram of the proposed method. Figure 1, which is based on three basic stages AHE and DCP algorithm, Lab colour model and reverse transformation and enhancement image, as follows.

#### AHE and DCP algorithm

The AHE and CLAHE are adaptive histogram equalization techniques used for contrast enhancement; CLAHE introduces a limitation on the amount of contrast enhancement to avoid over-amplification of noise, making it more suitable for a wider range of images, especially those with varying levels of detail and noise. The CLAHE technique; the image is split into several, nearly identical-sized, non-overlapping parts. Next, the graph for every region is computed. We obtain the segment term for cutoff graphs.

Professional redistribution is applied to each histogram to ensure that its height remains under the segment limit. The section term, which is provided by [12], is obtained by:

$$\beta = \frac{MN}{L} \left( 1 + \frac{\alpha}{100} (S_{max} - 1) \right) \quad (1)$$

where:  $L$  is the number of grayscales,  $MN$  is the number of pixels in each region, and  $\beta$  is the clip limit.

From Equation 17, the maximum allowed slope is denoted by  $S_{max}$ ,  $\alpha$  represents a clip factor, and if  $\alpha = 0$ , the clip limit is equal to  $MN/L$ . The relationship below can be used to show the general attenuation model that characterizes a physically hazy outdoors in aerial images [13]:

$$f(v) = I(v)t_r(v) + Ac(1 - T_r(v)) \quad (2)$$

where:  $I$  is the scene’s brightness and  $f$  is the intensity of the hazy image.  $T_r$  is the transmission channel, while  $Ac$  is the ambient light. The attenuation model is solved using the DCP technique, which enhances aerial or dusty images.  $I_i$  is provided by [13] at a very low intensity in one of the RGB components.

$$I_{dark}(v) = m \min_{i \in \{r,g,b\}} \left( \min_{y \in R(v)} (I_i(y)) \right) \quad (3)$$

where:  $R(v)$  represents the local patch’s center coordinate, and  $I_i(y)$  stands for the three channels red, green, and blue of  $i$ .

The DCP method reduces, consequently, the lightness of the  $I_i(y)$  dark channel. In Eq. 3 For each pixel in the image, calculate the minimum of the intensity values in a local patch around that pixel. This results in a dark channel image where each pixel value represents the minimum

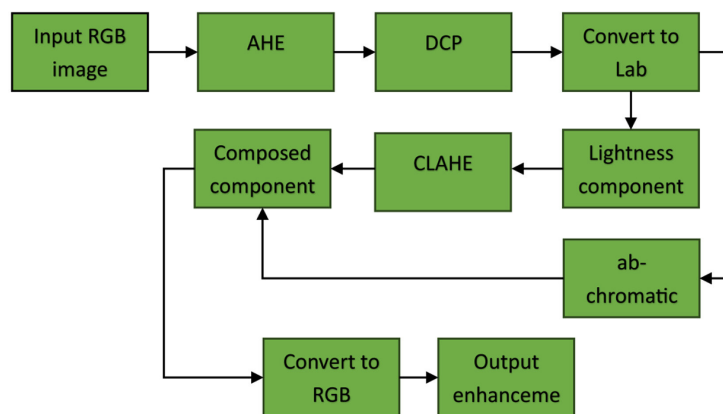


Figure 1. Steps of the suggested algorithm

intensity in its corresponding local patch, which appears outside and is absent of haze (except in bright areas), can be described as follows:

$$I_{dark}(v) \cong 0 \tag{4}$$

Consequently, the value of the transmission component can be obtained by [13]:

$$T_r(v) = 1 - d_{\min_{y \in R(v)}} \left( \min_{i \in (r,g,b)} \frac{J(y)}{Ac} \right) \tag{5}$$

A transmission can be improved by soft mapping. The image seems unusual if the haze or dust is removed. The ambient light (ideal value) is  $Ac=0.1$ , with a patch size of  $(15 \times 15)$  [13], and the value therefore is  $0 < Ac < 1$ , where  $d$  is set to 0.95 [13]. Next, provides an enhanced image.

$$I(v) = \frac{j(v)-Ac}{\max(T_r(v),0.1)} + Ac \tag{6}$$

### Lab colour model

We use the lab colour model to improve the lighting component using AHE without affecting the colour components. We convert the RGB space to the Lab space using the following Equation [14]:

$$\begin{bmatrix} X \\ Y \\ Z \end{bmatrix} = \begin{bmatrix} 0.41 & 0.35 & 0.18 \\ 0.21 & 0.71 & 0.07 \\ 0.01 & 0.11 & 0.95 \end{bmatrix} \cdot \begin{bmatrix} r'(x,y) \\ g'(x,y) \\ b'(x,y) \end{bmatrix} \tag{7}$$

$$f(r) = \begin{cases} \sqrt[3]{r} & \text{for } r > e \\ 7.787r + \frac{16}{116} & \text{for } r \leq e \end{cases} \tag{8}$$

$$L^* = \begin{cases} 116 \left( \frac{Y}{Y^n} \right) \frac{Y}{Y^n} > e \\ 903.3 \left( \frac{Y}{Y^n} \right) \frac{Y}{Y^n} \leq e \end{cases} \tag{9}$$

$$a^* = 500 \left( f \left( \frac{X}{X^n} \right) - f \left( \frac{Y}{Y^n} \right) \right) \tag{10}$$

$$b^* = 200 \left( f \left( \frac{Y}{Y^n} \right) - f \left( \frac{Z}{Z^n} \right) \right) \tag{11}$$

where:  $e = 0.008856$  [14], it is preferred for the stretched values

$$Le = \frac{L-L_{min}}{L_{max} - L_{min}} \tag{12}$$

### Reverse transformation and enhancement image

To obtain the image colour, we reverse convert from Lab to RGB according to the following Equation [15]:

$$L_{ne} = L_e \times 100 \tag{13}$$

$$X = X_n \left\{ \begin{array}{l} \left( \frac{L^*}{166} + \frac{a^*}{500} + \frac{16}{166} \right)^3 \text{ if } L^* > h \\ \frac{1}{7.787} \left( \frac{L^*}{116} + \frac{a^*}{500} \right) \text{ if } L^* \leq h \end{array} \right\} \tag{14}$$

$$Y = Y_n \left\{ \begin{array}{l} \left( \frac{L^*}{116} + \frac{16}{166} \right)^3 \text{ if } L^* > h \\ \frac{1}{7.787} \frac{L^*}{116} \text{ if } L^* \leq h \end{array} \right\} \tag{15}$$

$$Z = Z_n \left\{ \begin{array}{l} \left( \frac{L^*}{116} - \frac{b^*}{200} + \frac{16}{116} \right)^3 \text{ if } L^* > h \\ \frac{1}{7.787} \left( \frac{L^*}{116} - \frac{b^*}{200} \right) \text{ if } L^* \leq h \end{array} \right\} \tag{16}$$

where:  $h = 7.9996$ , and then:

$$\begin{bmatrix} R \\ G \\ B \end{bmatrix} = \begin{bmatrix} 3.22 & -1.51 & -0.49 \\ -0.96 & 1.87 & 0.04 \\ 0.07 & -0.20 & 1.05 \end{bmatrix} \cdot \begin{bmatrix} X \\ Y \\ Z \end{bmatrix} \tag{17}$$

### IMAGE QUALITY ASSESSMENT

Image quality assessment is the act of quantifying an image’s perceived quality. Various methods and metrics are utilized, depending on the specific quality aspects under evaluation. Here are some common approaches, Subjective Assessment: This method entails human observers rating image quality based on their perception. While providing the most accurate measure, it can be time-consuming and costly. Objective assessment: Objective metrics quantify image quality without human judgment, using mathematical models that simulate aspects of human perception, which are divided into two types of quality standards, reference and non-reference

### Entropy

Entropy was used to measure the quality of the images, and a higher value indicated an increase in quality, and when the value decreased, a decrease in quality was indicated. Entropy applied to the probability density function at the intensity level  $p(I)$  can measure the quality of colour images received with respect to [16]:

$$E(I) = -\sum_{l=0}^{l-1} p(I) \log p(I) \tag{18}$$

where:  $I$  represents the total number of gray levels.

### Mean of the standard deviation

The mean of the standard deviation (MSD) is employed to assess lightness and contrast while The standard deviation ( $\sigma$ ) is used to evaluate in general contrast [17]:

$$\sigma = \sqrt{\sum_{i=1}^M \sum_{j=1}^N \left(\frac{X(i,j)}{MN}\right) - (\mu)^2} \quad (19)$$

The symbol  $X(i, j)$  represents the value of a pixel.  $M$  and  $N$  stand for the columns and rows of the image, respectively. The mean of the image is denoted by  $(\mu)$ . Image contrast rises with rising standard deviation levels. Making Use of the Mean The contrast and lightness were computed using the standard deviation (MSD), as indicated below:

$$\bar{\sigma} = \frac{\sigma}{r} \quad (20)$$

where:  $r$  is the number of local regions.

### Structural similarity index metric

The degree to which the original data was maintained was assessed using reference metrics such as structural similarity index metric (SSIM) [18]. The degree of similarity between the processed image  $y$  and the original image  $x$  is determined by the structural similarity index metric:

$$SSIM = \frac{(2\mu_x\mu_y + \alpha_1)(2\sigma_{xy} + \alpha_2)}{\mu_x^2 + \mu_y^2 + \alpha_1(\sigma_x^2 + \alpha_2)} \quad (21)$$

### Perception-based image quality evaluator

The perception-based quality estimator (PIQE) predicts quality by extracting local features from perceptually significant spatial regions. The PIQE for quantification is [19]:

$$PIQE = \frac{(\sum_{k=1}^{N_{SA}} D_{sk}) + C_1}{(N_{SA} + C_1)} \quad (22)$$

where:  $D_{sk}$  is the amount of distortion allocated for the block and  $N_{SA}$  refers to the number of spatially active blocks in the main binary image space.  $C_1$  is a positive constant included to prevent numerical instability.

## RESULTS

In this study, we enhanced microscopic images using a proposed method, which utilized 50 JPG-type microscopy images from [20]. To assess the effectiveness of this method, we compared it with other methods (RACR [6], AHEFL [11], FLSMF [2], MMBSICHE [10], PCAURM [9], and MCHE [8]) using both reference and non-reference quality standards (EN, MSD, SSIM, and PIQE). The evaluation results, presented in Table 1, demonstrate that our method yielded the best improvements. The proposed method obtained the highest values in general for the EN, MSD and SSIM scale, which indicates its success in increasing contrast without distorting the original lighting information, and the second lowest value for the PIQE colour scale, which indicates the success of the proposed method in retrieving colour information after improvement. Figure 2 displays a selection of four images from the dataset, serving as a detailed model. These images are further analysed in Table 2, which lists the quality values for the four selected images, confirming the superiority of our method. Additionally, Figure 3 showcases an image that was enhanced using our method, along with previous methods for comparison. Histograms for Figure 1 and 2, as shown in Figures 4 and 6, illustrate the various improvements made, indicating the favourable distribution rates achieved by our method. Moreover, Figures 5 and 7 depict areas that were enlarged to assess the enhancement's impact on marginal areas, focusing in Figure 2 and 4, which

**Table 1.** Average quality assessment for data (50 images)

Method	EN	MSD	SSIM	PIQE
SUG	7.913	61.04	0.760	35.324
RACR (2022)	7.377	56.852	0.545	36.431
AHEFL (2023)	7.967	62.809	0.550	36.614
FLSMF (2020)	7.603	56.837	0.651	35.445
MMBSICHE (2015)	7.651	42.829	0.9134	32.735
PCAURM (2021)	7.676	51.067	0.881	36.886
MCHE (2015)	7.678	59.757	0.693	34.463



**Table 2.** The qualities for enhanced images (a, b, c & d)

Image_1					Image_2				
Method	EN	MSD	SSIM	PIQE	METHOD	EN	MSD	SSIM	PIQE
SUG	7.700	69.753	0.314	39.125	SUG	7.799	73.622	0.601	26.717
RACR	7.518	59.245	0.516	40.052	RACR	7.419	69.495	0.644	45.719
AHEFL	7.988	65.104	0.515	45.451	AHEFL	7.995	68.284	0.663	37.058
FLSMF	7.704	57.773	0.594	41.990	FLSMF	7.775	68.782	0.778	41.454
MMBSICHE	7.768	42.529	0.930	40.172	MMBSICHE	7.890	56.344	0.937	36.096
PCAURM	7.884	55.919	0.875	44.246	PCAURM	7.873	62.284	0.917	39.407
MCHE	7.679	63.336	0.753	41.573	MCHE	7.725	67.243	0.819	36.026
Image_3					Image_4				
Method	EN	MSD	SSIM	PIQE	METHOD	EN	MSD	SSIM	PIQE
SUG	7.803	70.397	0.428	28.974	SUG	7.833	73.136	0.471	27.699
RACR	7.431	56.530	0.455	32.196	RACR	7.411	68.874	0.516	42.590
AHEFL	7.988	63.804	0.481	34.222	AHEFL	7.997	68.811	0.5271	39.446
FLSMF	7.565	55.201	0.506	28.542	FLSMF	7.617	66.305	0.639	42.716
MMBSICHE	7.639	38.790	0.907	27.264	MMBSICHE	7.785	52.326	0.914	39.919
PCAURM	7.731	47.332	0.885	30.469	PCAURM	7.895	62.373	0.878	39.266
MCHE	7.669	62.962	0.657	31.650	MCHE	7.677	67.921	0.831	40.647

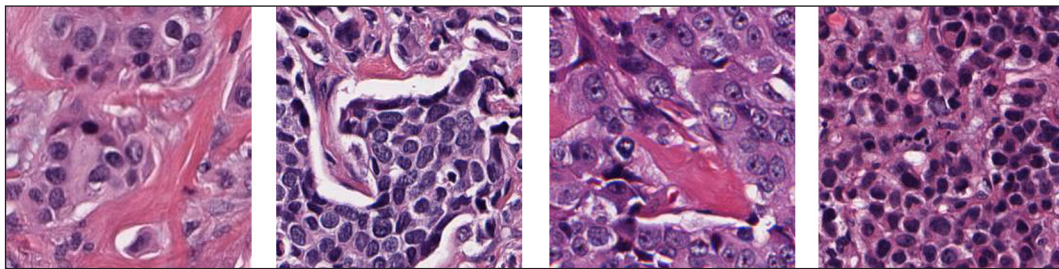


**Figure 2.** Four images selected from the data used

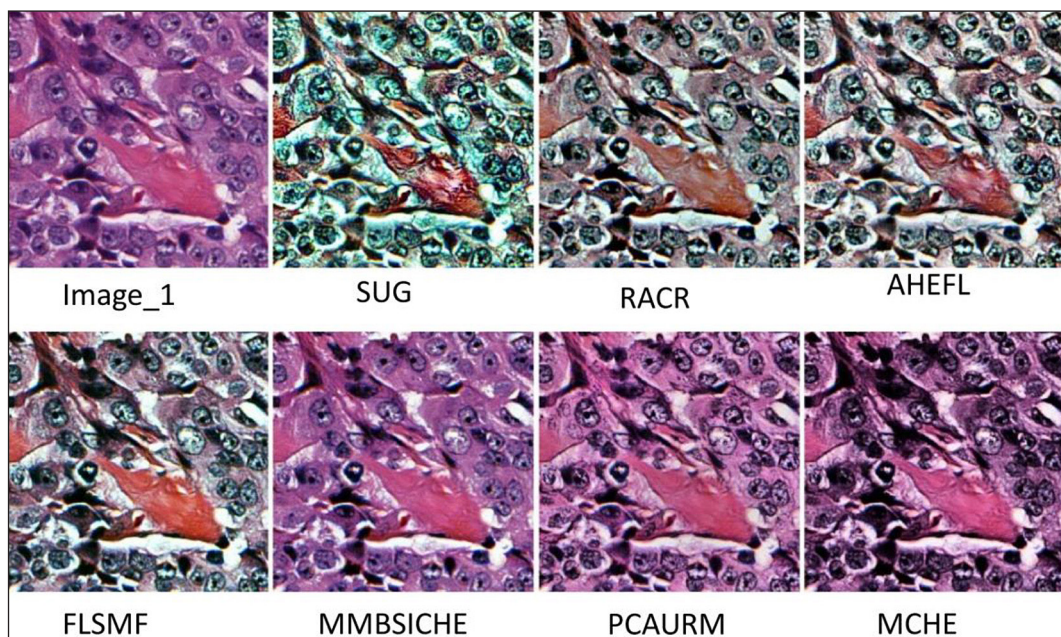


**Figure 3.** Image 1 is enhanced by various methods

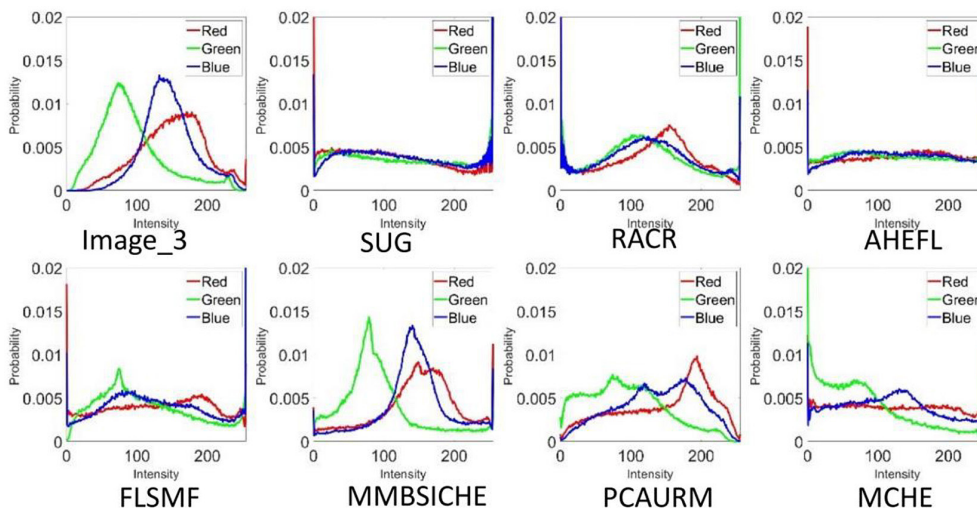


Figure 4. Histogram of image 1 enhanced by various methods

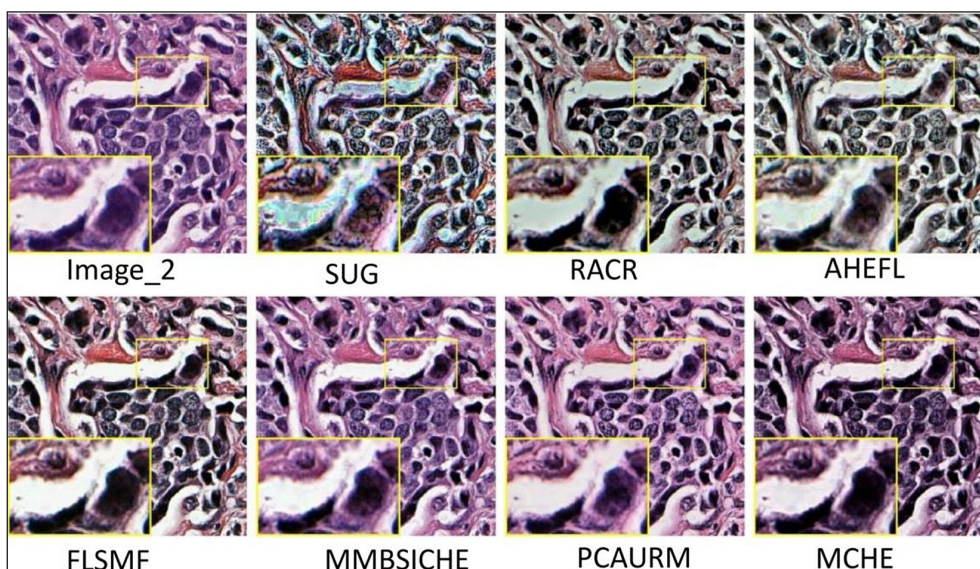


Figure 5. Comparisons of microscope image 2 enhancement results with zoom details

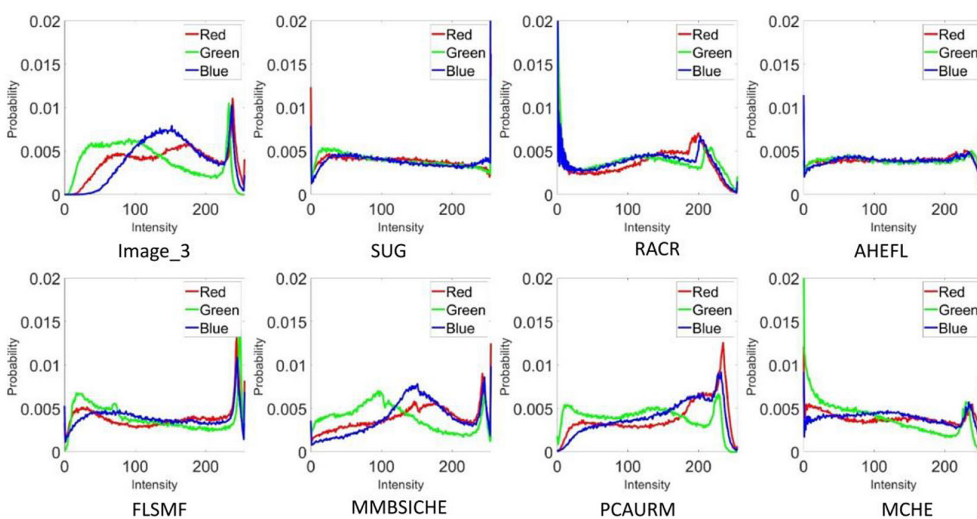


Figure 6. Histogram of image 2 enhanced by various methods



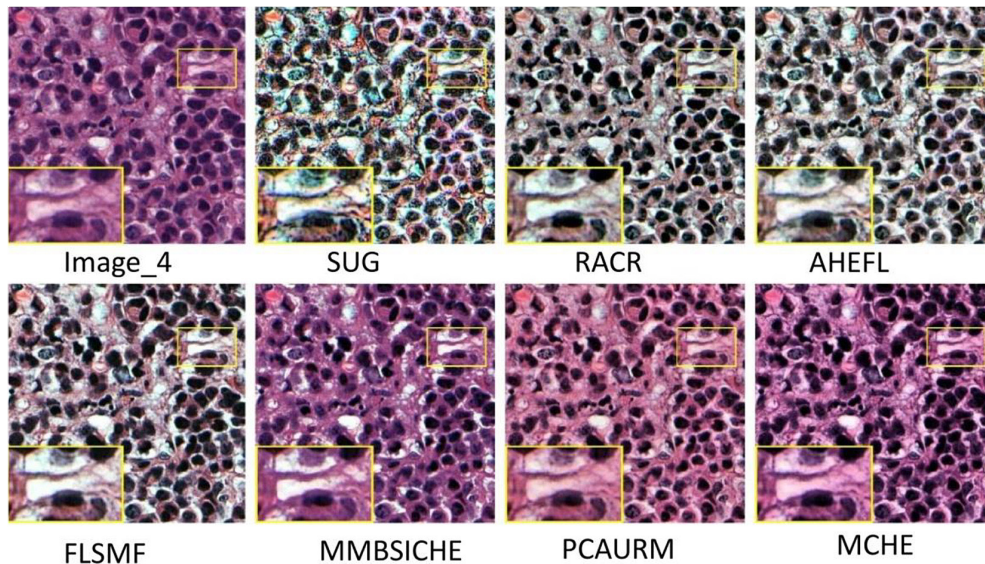


Figure 7. Comparisons of microscope image 4 enhancement results with zoom details

were improved by all algorithms. Our observation indicates that our proposed method effectively enhances marginal areas, maintaining the original image’s lighting without introducing distortion.

## CONCLUSIONS

The proposed algorithm enhanced microscopic images in this study by utilizing the DCP and AHE algorithms. The LAB colour model was employed to improve the lighting component. This approach was compared with several others (RACR, AHEFL, FLSMF, MMBSICHE, PCAURM, and MCHE) using reference and non-reference quality standards (EN, MSD, SSIM, and PIQE). The results demonstrated the effectiveness of the proposed method in enhancing microscopic images by improving the lighting component without introducing any colour distortions, as a future study, the proposed method can be developed to improve x-ray images.

## REFERENCES

1. Jain A.K. Fundamentals of Digital Image Processing. Englewood Cliffs, NJ, USA: Prentice-Hall, 1989.
2. Daway H., Daway E., Kareem H. Colour image enhancement by fuzzy logic based on sigmoid membership function, *Int. J. Intell. Eng. Syst.*, 2020, 13(5): 238–246.
3. Mohammed, M.H., Daway, H.G., Jouda, J. Automatic Cytoplasm and Nucleus detection in the white blood cells depending on hisogram analysis. In *IOP Conference Series: Materials Science and Engineering*. 2020, 871(1): 012071. IOP Publishing.
4. Razzak A., Hashem A. Facial expression recognition using hybrid transform, *Int. J. Comput. Appl.*, 2015, 119(15).
5. Hashim A., Daway H., Kareem H. No reference Image Quality Measure for Hazy Images. *Int. J. Comput. Appl.*, 2020, 13(6).
6. Daway, Esraa G., Abdulameer F.S., Daway H.G. X-ray image enhancement using retinex algorithm based on Colour restoration. *J. Eng. Sci. Technol.*, 2022, 17(2): 1276–1286.
7. Zhou, M., Jin K., Wang S., Ye J., Qian D. Colour retinal image enhancement based on luminosity and contrast adjustment. *IEEE Transactions on Biomedical Engineering*, 2017, 65(3): 521–527.
8. Hsu, W.Y., Chou, C.Y. Medical image enhancement using modified Colour histogram equalization. *Journal of Medical and Biological Engineering*, 2015, 35: 580–584.
9. Singh, N., Bhandari, A.K. 2021. Principal component analysis-based low-light image enhancement using reflection model. *IEEE Transactions on Instrumentation and Measurement*, 2021, 70: 1–10.
10. Singh, K., Kapoor, R. Image enhancement via median-mean based sub-image-clipped histogram equalization. *Optik*, 125(17): 4646–4651. Alization. *Journal of Medical and Biological Engineering*, 2015, 35: 580–584.
11. Kadhim, Ahlam M., Daway H.G. Enhancement of Microscopy Images by Using a Hybrid Technique Based on Adaptive Histogram Equalisation and Fuzzy Logic. *International Journal of Intelligent Engineering & Systems*, 2023, 16(1).



12. Zuiderveld, K. Contrast Limited Adaptive Histogram Equalization. *Graphic Gems IV*. San Diego: Academic Press Professional, 1994, 474–485.
13. He K., Sun J., Tang X. Single image haze removal using dark channel prior, *IEEE Trans. Pattern Anal. Mach. Intell.*, 2010, 33(12): 2341–2353.
14. Ebner M. *Colour constancy*, John Wiley and Sons, 2007, 7.
15. Reinhard E., Khan E., Akyuz A., Johnson G. *Colour imaging: fundamentals and applications*, CRC Press, 2008.
16. Gonzalez R.C., Woods R.E., Eddins S.L. *Digital Image Processing Using MATLAB*. New Jersey, Prentice Hall, 2003.
17. Hashim A.R., Daway H.G., Kareem H.H. Single image dehazing by dark channel prior and luminance adjustment, *Imaging Sci. J.*, 2020, 68(5–8): 278–287.
18. Zhou W., Bovik A.C., Sheikh H.R., Simoncelli E.P. Image Quality Assessment: From Error Visibility to Structural Similarity. *IEEE Transactions on Image Processing*, 2004, 13(4): 600–612.
19. Venkatanath N., Praneeth D., Bh, M.C., Channappayya S.S., Medasani S.S. 2015. blind image quality evaluation using perception based features. in 2015 twenty first national conference on communications.
20. <https://www.kaggle.com/datasets/gangadhar/nuclei-segmentation-in-microscope-cell-images>.